A Bayesian assessment of the PCB temporal trends in Lake Erie fish communities

Somayeh Sadraddini [a], M. Ekram Azim [a], Yuko Shimoda [a], Satyendra P. Bhavsar [b,c], Ken G. Drouillard [d], Sean M. Backus [e], George B. Arhonditsis [a,c,*]

[a] Ecological Modeling Laboratory, Department of Physical and Environmental Sciences, University of Toronto, Toronto, Ontario, Canada M1C 1A4
[b] Ontario Ministry of Environment, Environmental Monitoring and Reporting Branch, Toronto, Ontario, Canada M9P 3V6
[c] Centre for Environment, University of Toronto, Toronto, Ontario, Canada M5S 3E8
[d] Great Lakes Institute for Environmental Research, University of Windsor, Windsor, Ontario, Canada N9B 3P4
[e] Water Quality Monitoring & Surveillance Division, Water Science and Technology Directorate, Environment Canada, Burlington, Ontario, Canada L7R 4A6

A B S T R A C T

The temporal trends of polychlorinated biphenyls (PCBs) in Lake Erie fish were evaluated using 30 years of fish contaminant data (1977–2007). The first step of our statistical analysis was based on simple exponential decay models parameterized with Bayesian inference techniques to assess the declining rates in four intensively sampled fish species, i.e., walleye (Stizostedion vitreum), coho salmon (Oncorhynchus kisutch), rainbow trout (Oncorhynchus mykiss) and white bass (Morone chrysops). Because the exponential model postulates monotonic decrease of the PCB levels, we included first- or second-order random error terms in our statistical formulations to accommodate non-monotonic patterns in the dataset studied. Generally, our results suggest that the PCBs have been decreasing over the last 30 years with relatively weak rates that vary among the different fish species examined. Yet, our analysis with the exponential decay model also identified an increasing trend in the PCB concentrations of walleye skinless–boneless filet data, which is manifested after the mid-90s. In the second step, we used dynamic linear modeling (DLM) analysis to account for the fact that the fish length covaries with the PCB concentrations and that different sized fish may have been sampled over time. Our DLM analysis suggests that the previously reported trend of the walleye filet data is actually an artifact associated with the bias of the fish sampling practices followed. The coho salmon and rainbow trout PCB concentrations have been decreasing steadily during the study period but the associated rates were relatively weak. Finally, the PCB trends in white bass appear to have been stabilized over that last decade, although the robustness of this result remains to be confirmed due to the temporal inconsistencies of the information used. We conclude by emphasizing the importance of explicitly accounting for the different covariates (e.g., length, age, lipid content) that can potentially hamper the detection of the actual temporal trends of fish contaminants.

© 2011 International Association for Great Lakes Research. Published by Elsevier B.V. All rights reserved.

Introduction

Among the bioaccumulative, toxic and persistent organic pollutants (POPs), polychlorinated biphenyls (PCBs) are of particular concern and historically have restricted the use of valuable commercial and recreational fishery resources in the Great Lakes. PCBs were first traced in the Great Lakes in the 1930s and their concentrations peaked in the late 1960s-early 1970s (Tanabe, 1988). As a result, PCB contamination was identified as a major threat to the integrity of the aquatic biota in the Great Lakes area. There has also been a growing concern that individuals who eat considerable amount of fish from the Great Lakes have greater exposure to toxic chemicals (Cole et al., 2004; Johnson et al., 1999). Consumption of Great Lakes sport fish has been one of the significant determinants of PCB burden in the human body (Humphrey, 1988; Tee et al., 2003). The reported human health risks from PCBs involve susceptibility to cardiovascular problems including coronary heart disease (Tomasallo et al., 2010), decreased verbal learning and increased depression (Fitzgerald et al., 2008), neurobehavioral alterations, motor immaturity, hyporeflexia, and lower psychomotor scores (Faroon et al., 2000), alterations/disruptions of thyroid stimulating hormone, triiodothyronine, thyroxine and sex steroid hormone functions (Turyk et al., 2006) and diabetes (Turyk et al., 2009a, 2009b). Thus, while the health benefits of fish consumption are widely advocated, the potential human health impacts from the worrisome PCB levels underscore the importance of meticulously updating the fish consumption advisories typically issued by the Ontario Ministry of the

* Corresponding author at: Ecological Modeling Laboratory, Department of Physical and Environmental Sciences, University of Toronto, Toronto, Ontario, Canada M1C 1A4. Tel.:+1 416 208 4858.
E-mail addresses: somayeh.sadraddini@utoronto.ca (S. Sadraddini), eazim@utsc.utoronto.ca (M.E. Azim), yshimoda@utsc.utoronto.ca (Y. Shimoda), Satyendra.Bhavsar@ontario.ca (S.P. Bhavsar), kgd@uwindsor.ca (K.G. Drouillard), Sean.Backus@ec.gc.ca (S.M. Backus), georgea@utsc.utoronto.ca (G.B. Arhonditsis).

Environment and different US state governments in the Great Lakes area.

Responding to increased public pressure and advocacy for virtual elimination of persistent toxic pollutants from the Great Lakes, various regulatory actions were undertaken at different government levels. *PCB* production was effectively banned in the 1970s in North America. The Great Lakes Water Quality Agreement (*GLWQA*) between Canada and USA was signed in 1972 and was subsequently revised in 1978. The agreement included a call for monitoring and research programs to identify the spatiotemporal contaminant trends in the sediments and biota (IJC, 1978, 2006). Implementation of these regulatory actions resulted in decreased levels of most contaminants in the Great Lakes fish through the 1980s, but the rate of decrease in fish are reported to have diminished since the early 1990s; especially in Lake Erie (Bhavsar et al., 2007; Carlson et al., 2010). The reasons for these trends are not fully known, but existing mechanistic explanations include the food web alterations induced from invasive species in the Great Lakes (Hogan et al., 2007; Morrison et al., 1998) and also shifts in the trophodynamics associated with global warming (French et al., 2006).

The reported contaminant trends could have also been influenced by many factors such as the type of statistical analysis performed, data pooling across locations, type of samples (whole fish vs. filet portions), seasonality, and lack of explicit consideration of important covariates such as the fish size, age, feeding habits, behavioral patterns, reproductive status, growth and lipid content. Inappropriate data analysis and interpretation of statistical trends derived from incomplete information can conceivably provide misleading results. Therefore, holistic modeling frameworks that explicitly incorporate all the causal factors are essential to delineate the actual contaminant trends and to elucidate the underlying mechanisms. To this end, different modeling strategies have been used to assess the trajectories of the historical fish contaminant data. Stow et al. (2004) analyzed lake trout *PCBs* from Lake Michigan with dynamic linear modeling and Bayesian model averaging (*BMA*) of four individual models: exponential decay model, exponential decay model with a nonzero asymptote, double exponential model and mixed order model. Hickey et al. (2006) evaluated the temporal trends of chlorinated organic contaminants in Great Lakes trout and walleye using the single exponential decay model and the double exponential model that distinguishes between fast and slow decay processes, while both approaches explicitly accounted for the presence of a stable contaminant source resulting in an irreducible or baseline concentration. Similarly, a recent analysis by Gewurtz et al. (2010) used exponential decay models to examine the spatiotemporal trends of organochlorines and mercury in fish species from the St. Clair River/Lake St. Clair corridor. Finally, Bhavsar et al. (2010) used General Linear Model Univariate analysis with Tukey's posthoc multiple comparison along with the non-parametric Mann–Kendal test to detect *Hg* trends in time and space of lake trout and walleye in Lakes Superior, Georgian Bay, Huron, Erie and Ontario during the 1980–1990 and 2000–2007 periods.

In this study, we have undertaken a systematic and rigorous trend analysis based on a 30-yr dataset of *PCB* concentrations in fish from Lake Erie. Our aim is to illustrate a Bayesian methodological framework that can objectively detect the temporal trends of fish contaminant concentrations. In the first step, we use single exponential decay models to assess the declining rates in four intensively sampled fish species, i.e., walleye (*Stizostedion vitreum*), coho salmon (*Oncorhynchus kisutch*), rainbow trout (*Oncorhynchus mykiss*) and white bass (*Morone chrysops*). Because the exponential decay model postulates monotonic decrease of the *PCB* levels, we include first- or second-order random walk error terms to accommodate the likelihood of non-monotonic patterns in the time series data. In the second step, we use dynamic linear modeling to verify the temporal trends derived from the first phase of our statistical framework by explicitly accounting for the covariance between *PCB* concentrations and fish length (Stow et al., 2004). Our study also revisits the capacity of several of the hypotheses proposed in the literature to explain the temporal *PCB* trends in Lake Erie fish communities. Finally, we conclude by underscoring that all modeling frameworks aiming to impartially identify the actual temporal trends of fish contaminants should explicitly examine the role of the different covariates (e.g., length, gender, lipid content, weight, season, location) and thus

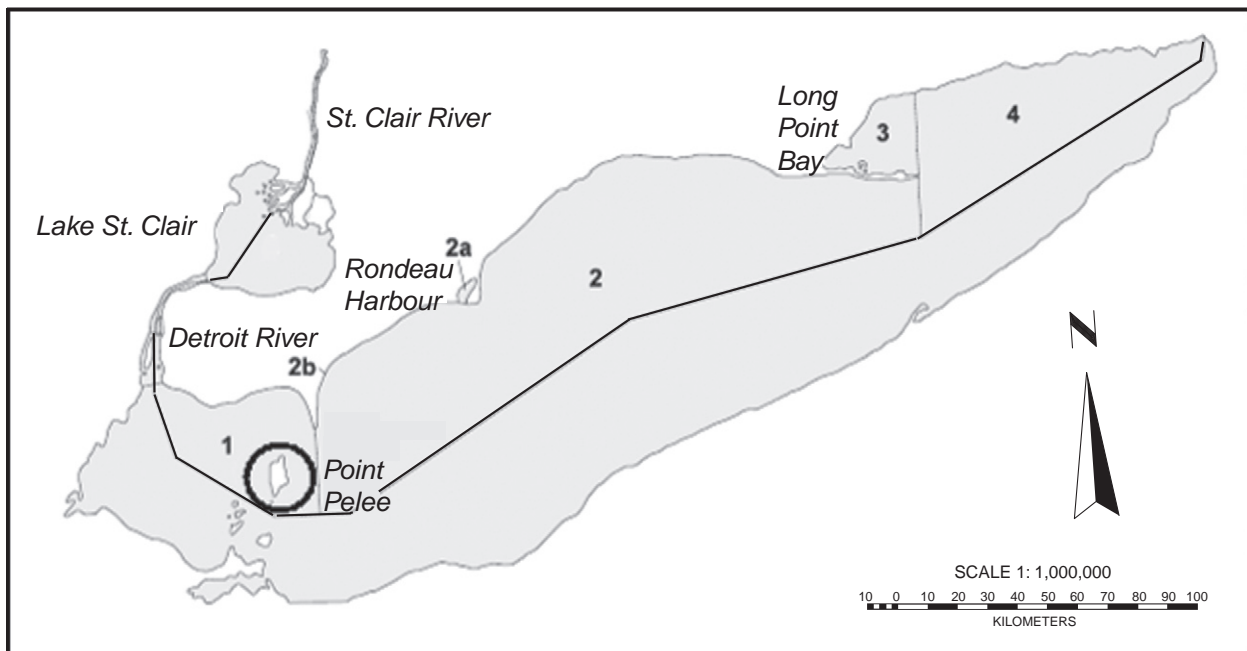**Fig. 1.** Map of Lake Erie with the four sampling sites: *1*: Western Basin, *2*: Central Basin, *3*: Long Point Bay, and *4*: Eastern Basin. The area around Pelee Island (black circle) represents the federal (Environment Canada) sampling location.

Table 1
Basic statistics of PCB concentrations (ng/g wet weight) in walleye whole fish data and in skinless–boneless filet data from walleye, coho salmon, rainbow trout and white bass in Lake Erie.

Species	N	Mean	SD	Median	Inter quart.	Skewness	Kurtosis
Walleye (WF) Stizostedion vitreum	969	1329	987	1100	900	2.42	9.66
Walleye (SBF) Stizostedion vitreum	899	114	119	80	105	2.79	1.93
Coho salmon Oncorhynchus kisutch	694	463	251	410	311	1.18	2.87
Rainbow trout Oncorhynchus mykiss	302	399	291	326	350	1.58	5.14
White bass Morone chrysops	1165	309	245	240	264	1.84	4.37

control the possible bias introduced by the typical sample collection practices and/or changes in other ecological parameters.

Methods

The present study is based on the provincial (Ontario Ministry of the Environment; OMOE, Canada) dorsal filet measurements used for fish consumption advisories, and the federal (Environment Canada; EC) whole fish measurements used to assess overall environmental contamination and risk to fish and fish-consuming wildlife (Bhavsar et al., 2010). In our analysis, the selection of fish species was driven by the data availability and their ecological/commercial importance. We examined four intensively sampled species, i.e., walleye (S. vitreum), coho salmon (O. kisutch), rainbow trout (O. mykiss) and white bass (M. chrysops). The examination of the PCB trends was based on whole

fish (WF) and skinless–boneless filet (SBF) samples for walleye and only SBF samples for the remaining fish species. The whole-fish samples were collected from Pelee Island in the western part of Lake Erie, while the filet samples were pooled from four sites on the Canadian side, i.e., western basin, central basin, Long Point Bay, and eastern basin (Fig. 1). The number of observations for each species is given in Table 1. The analytical procedure is described for the OMOE samples by Bhavsar et al. (2007) and for the EC samples by Borgmann and Whittle (1983).

Our modeling framework consists of two steps that aim to detect the presence of statistically significant non-monotonic trends associated with the fish PCB concentrations (step I), and to examine if these temporal trends are actually detected when we explicitly account for the covariance between PCB levels and fish length (step II). Bayesian inference was used as a means for estimating model parameters due to its ability to include prior information in the modeling analysis and to explicitly handle the model structure and parameter uncertainty (Gelman et al., 2004). Bayesian inference treats each parameter θ as random variable, and uses the likelihood function to express the relative plausibility of obtaining different values of this parameter when particular data have been observed:

$$\pi(\theta|data) = \frac{\pi(\theta)L(data|\theta)}{\int_\theta \pi(\theta)L(data|\theta)d\theta} \tag{1}$$

where $\pi(\theta)$ represents our prior statements regarding the probability distribution that more objectively depicts the existing knowledge on the θ values, $L(data|\theta)$ corresponds to the likelihood of observing the data given the different θ values, and $\pi(\theta|data)$ is the posterior probability that expresses our updated beliefs on the θ values after the existing data from the system are considered. The denominator in Eq. (1) is the expected value of the likelihood function, and acts as a

Table 2
Deviance information criterion, posterior mean values, 2.5% and 97.5% percentiles (italicized numbers) of the stochastic nodes of the models used to describe the temporal trends of PCB concentrations in walleye (both WF and SBF portions), coho salmon (SBF), white bass (SBF) and rainbow trout (SBF).

Models	Parameters[a]	Walleye WF	Walleye SBF	Coho Salmon SBF	White Bass SBF	Rainbow Trout SBF
Exponential model with 1st order smoothing	DIC	1788	2123	1132	2374	623
	PCB$_0$	*982*	*87*	*284*	*237*	*252*
		1054	164	386	277	325
		1131	*326*	*570*	*362*	*428*
	k	*−0.003*	*−0.089*	*−0.040*	*−0.027*	*−0.023*
		−0.001	−0.040	−0.013	−0.009	−0.007
		>−0.001[b]	*−0.003*	*>−0.001[b]*	*>−0.001[b]*	*>−0.001[b]*
	ω	*0.307*	*0.426*	*0.243*	*0.331*	*0.300*
		0.424	0.592	0.369	0.444	0.481
		0.581	*0.823*	*0.559*	*0.599*	*0.734*
	σ$_ε$	*0.572*	*0.740*	*0.510*	*0.635*	*0.602*
		0.599	0.776	0.538	0.661	0.653
		0.627	*0.814*	*0.568*	*0.689*	*0.709*
Exponential model with 2nd order smoothing	DIC	1789	2121	1128	2374	629
	PCB$_0$	*994*	*87*	*285*	*238*	*241*
		1062	161	388	274	301
		1137	*308*	*558*	*359*	*388*
	k	*−0.002*	*−0.086*	*−0.034*	*−0.026*	*−0.023*
		−0.001	−0.039	−0.010	−0.009	−0.007
		>−0.001[b]	*−0.002*	*>−0.001[b]*	*>−0.001[b]*	*>−0.001[b]*
	ω	*0.430*	*0.579*	*0.321*	*0.447*	*0.154*
		0.617	0.832	0.495	0.617	0.325
		0.860	*1.181*	*0.756*	*0.844*	*0.668*
	σ$_ε$	*0.572*	*0.741*	*0.509*	*0.635*	*0.612*
		0.599	0.777	0.537	0.662	0.667
		0.627	*0.814*	*0.567*	*0.689*	*0.727*

[a] DIC: Deviance Information Criterion; PCB$_0$: the PCB concentration at $t=0$; k: the decay coefficient; ω: the conditional standard deviation of the random error terms δ_t, representing the annual discrepancies from the trajectory delineated by the common exponential decay model; and σ$_ε$: the measurement standard error.
[b] Denotes a negative value very close to zero.
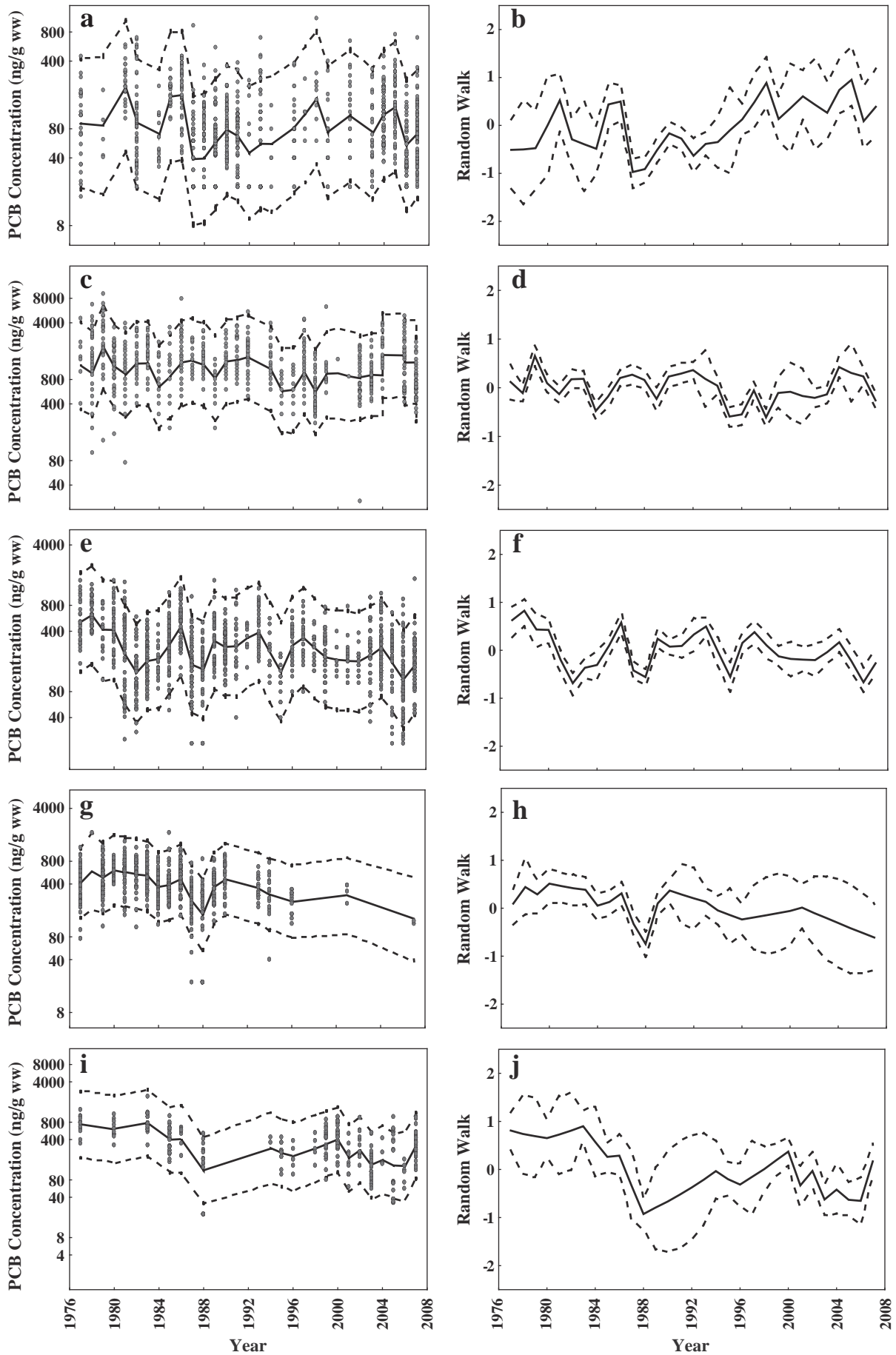
scaling constant that normalizes the integral of the area under the posterior probability distribution.

Step I — exponential decay models with random walk terms

The first step of the analysis was based on the exponential decay model (Stow et al., 2004):

$$PCB_t = PCB_0 e^{kt} + \delta_t + \varepsilon \qquad (2)$$

where PCB_t is the PCB concentration in year t; PCB_0 is the PCB concentration at $t = 0$; k is the decay coefficient. A fundamental weakness of the simple exponential decay model is the postulation of a monotonic decrease of the PCB levels, and therefore its inability to capture systematic deviations from this trend. To accommodate possible non-monotonic patterns in the time series data, we included (zero mean) random error terms δ_t representing the annual deviations from the trajectory delineated by the common exponential decay model. To reflect the prior belief that these annual discrepancies are correlated, we assumed a first-order random walk prior specified as (Arhonditsis et al., 2008a,b; Shaddick and Wakefield, 2002):

$$p\left(\delta_t \mid \delta_{-t}, \omega^2\right) \sim \begin{cases} N\left(\delta_{t+1}, \omega^2\right) & \text{for } t = 1 \\ N\left(\dfrac{\delta_{t-1} + \delta_{t+1}}{2}, \dfrac{\omega^2}{2}\right) & \text{for } t = 2, \ldots, T-1 \\ N\left(\delta_{t-1}, \omega^2\right) & \text{for } t = T \end{cases} \qquad (3)$$

where δ_{-t} denotes all elements of δ_t except from the error associated with a particular year t, ω^2 is the conditional variance and the prior density $p(\omega^2)$ was based on a conjugate inverse-gamma (0.001, 0.001) distribution. This statistical approach implies that the first-order differences of the annual PCB levels are smooth, and that the probability of sudden jumps between consecutive years is unlikely. Alternatively, we examined a second-order random walk prior for δ_t representing prior beliefs that the rate of change (gradient) of the PCB concentrations over the study period was smooth:

$$p\left(\delta_t \mid \delta_{-t}, \omega^2\right) \sim \begin{cases} N\left(2\delta_{t+1} - \delta_{t+2}, \omega^2\right) & \text{for } t = 1 \\ N\left(\dfrac{2\delta_{t-1} + 4\delta_{t+1} - \delta_{t+2}}{5}, \dfrac{\omega^2}{5}\right) & \text{for } t = 2 \\ N\left(\dfrac{-\delta_{t-2} + 4\delta_{t-1} + 4\delta_{t+1} - \delta_{t+2}}{6}, \dfrac{\omega^2}{6}\right) & \text{for } t = 3, \ldots, T-2 \\ N\left(\dfrac{-\delta_{t-2} + 4\delta_{t-1} + 2\delta_{t+1}}{5}, \dfrac{\omega^2}{5}\right) & \text{for } t = T-1 \\ N\left(-\delta_{t-2} + 2\delta_{t-1}, \omega^2\right) & \text{for } t = T, \end{cases} \qquad (4)$$

Because of the added complexity, recent work by Azim et al. (2011) showed that the present statistical formulation is prone to poor parameter identification when coupled with more complex models (e.g., mixed-order model). In particular, the Azim et al. (2011) study noted that the predicted decay coefficients from the mixed-order model were accompanied by substantial standard deviations

(coefficients of variation ≈ 70–114%), which counterbalances the support provided by its higher performance relative to simpler models. Thus, our strategy was to select the simplest possible model structure (single exponential decay model) combined with the random walk term to quantify the decreasing rates as well as to detect deviations from this trend during the study period. Finally, the ε term represents the measurement error and is assumed to follow a Gaussian distribution, $N(0, \sigma_\varepsilon^2)$. Contrary to the time variant random error terms δ_t, the measurement error does not depend on time and the prior density $p(\sigma_\varepsilon^2)$ was again based on a conjugate inverse-gamma (0.001, 0.001) distribution.

Sensitivity analysis

The Bayesian configuration of the single exponential model was based on non-informative prior distributions for the parameters PCB_0 [$\sim N(0,10{,}000)I(0,)$] and k [$\sim N(0,10{,}000)I(,0)$], i.e., normal distributions with mean 0 and variance 10,000 constrained to sample positive and negative values, respectively. To determine the robustness of the results to this assumption, the first-order exponential decay model was also run using three different PCB_0 priors. Specifically, we used normal (*Prior 1*) and lognormal (*Prior 2*) parameter distributions parameterized such that 95% of the respective values lay within the minimum and maximum PCB concentrations in the first year examined, and a multivariate normal prior that accounts for the covariance between the parameters PCB_0 and k (*Prior 3*). [The WinBUGS codes associated with this sensitivity analysis exercise can be found in the Appendix.] Finally, we compared the impact of the specification $k \in [-\infty, 0]$ relative to the general characterization of $k \in [-\infty, +\infty]$, and the results were practically identical. The only difference was that the k marginal posteriors tended to be somewhat flatter due to the inclusion of the random walk term. Evidently, this separation of the space assigned to the k and δ_t terms alleviates the identification problem associated with the more complex structure of our statistical formulation.

Step II — dynamic linear modeling

In the next phase, dynamic linear modeling analysis was used to examine to what extent the PCB temporal trends detected in the first phase are actually manifested, if we explicitly account for the fact that the fish length covaries with the PCB concentrations and that unequal number of fish samples of different sizes may have been sampled over time. The main advantage of the DLMs is the explicit recognition of structure in the time series, i.e., the data are sequentially ordered and the level of the response variable at each time step is related to its levels at earlier time steps in the data series (Lamon et al., 1998; Stow et al., 2004). In contrast with regression analysis, parameter estimates are influenced only by prior and current information, not by subsequent data. Parameter values are dynamic and reflect shifts in both the level of the response variable and the underlying ecological processes. Using Bayes' Theorem, the DLM process updates our knowledge regarding the parameters with the likelihood of the data and our prior knowledge. DLMs easily handle missing values/unequally spaced data, and minimize the effect of outliers (Pole et al., 1994). All DLMs consist of an observation equation and a system equation (West and Harrison, 1989). In particular, the DLMs used herein were specified as follows:

Observation equation:

$$ln\,[PCB]_{ti} = level_t + \beta_t\, ln[length]_{ti} + \psi_{ti} \qquad \psi_{ti} \sim N[0, \Psi_t] \qquad (5a)$$

Fig. 2. Temporal trends of PCB concentrations (1977–2007) using the exponential decay model with (a, b) walleye skinless–boneless filet, (c, d) walleye whole fish, (e, f) white bass skinless–boneless filet, (g, h) coho salmon skinless–boneless filet, and (i, j) rainbow trout skinless–boneless filet data from Lake Erie. The circles indicate the measured values, while the solid and dashed lines correspond to the median and the 95% credible intervals of the posterior predictive distributions, respectively. The first-order random walk terms correspond to the δ annual values in Eq. (2) introduced to account for the structural deficiencies of the exponential decay model.

System equations:

$$level_t = level_{t-1} + rate_t + \omega_{t1} \qquad \omega_{t1} \sim N[0, \Omega_{t1}]$$
$$rate_t = rate_{t-1} + \omega_{t2} \qquad \omega_{t2} \sim N[0, \Omega_{t2}]$$
$$\beta_t = \beta_{t-1} + \omega_{t3} \qquad \omega_{t3} \sim N[0, \Omega_{t3}]$$
$$1/\Omega_{tj}^2 = \zeta^{t-1} \cdot 1/\Omega_{1j}^2, 1/\Psi_t^2 = \zeta^{t-1} \cdot 1/\Psi_1^2 \quad t > 1 \text{ and } j = 1 \text{ to } 3$$
$$level_1, rate_1, \beta_1 \sim N(0, 10000) \qquad t = 1$$
$$1/\Omega_{1j}^2, 1/\Psi_1^2 \sim gamma(0.001, 0.001)$$

(5b)

where $\ln[PCB]_{ti}$ is the observed lnPCB concentration at time t in the individual sample i; $level_t$ is the mean lnPCB concentration at time t when accounting for the covariance with the fish length; $\ln[length]_{ti}$ is the observed (standardized) fish length at time t in the individual sample i; $rate_t$ is the rate of change of the level variable; β_t is a length (regression) coefficient; ψ_t, ω_{tj} are the error terms for year t sampled from normal distributions with zero mean and variances Ψ_t^2, Ω_{tj}^2, respectively; the discount factor ζ represents the aging of information with the passage of time; $N(0, 10{,}000)$ is the normal distribution with mean 0 and variance 10,000; and $gamma(0.001, 0.001)$ is the gamma distribution with shape and scale parameters of 0.001. The prior distributions for the parameters of the initial year $level_1, rate_1, \beta_1, 1/\Omega_{1j}^2$, and $1/\Psi_1^2$ are considered "non-informative" or vague. In this study, we opted for a parsimonious *DLM* construct, in which the same discount factor was implemented on all the priors for the first year of the study, and therefore non-constant and data-driven variances (with respect to time) were introduced without having to estimate a large number of parameters. Namely, we examined different discounts between 0.9 and 1.0 and the results reported here are based on a discount value of 0.95. Discounts were selected by conducting a model search, in which models with different discount factors were compared on the basis of their difference in $\log_e$ likelihoods (Lamon et al., 1998).

Model computations

Sequence of realizations from the model posterior distributions were obtained using Markov Chain Monte Carlo (*MCMC*) simulations (Gilks et al., 1998). Specifically, we used the general normal-proposal Metropolis algorithm as implemented in the WinBUGS software; this algorithm is based on a symmetric normal proposal distribution, whose standard deviation is adjusted over the first 4000 iterations, such as the acceptance rate ranges between 20% and 40%. We used three chain runs of 80,000 iterations and samples were taken after the *MCMC* simulation converged to the true posterior distribution. Convergence was assessed using the modified Gelman–Rubin convergence statistic (Brooks and Gelman, 1998). Generally, we noticed that the sequences converged very rapidly (≈ 1000 iterations), and the summary statistics reported in this study were based on the last 75,000 draws by keeping every 20th iteration (thin = 20) to avoid serial correlation. The accuracy of the posterior parameter values was inspected by assuring that the Monte Carlo error for all parameters was less than 5% of the sample standard deviation.

Model comparisons

The models presented in this analysis were compared using the deviance information criterion (*DIC*), a Bayesian measure of model fit and complexity (Spiegelhalter et al., 2002). *DIC* is given by

$$DIC = \overline{D(\theta)} + p_D \qquad (7)$$

where $\overline{D(\theta)}$ is the posterior mean of the deviance, a measure of residual variance in data conditional on the parameter vector θ. The

deviance is defined as $-2\log(\text{likelihood})$ or $-2\log[p(y|\theta)]$; p_D is a measure of the "effective number of parameters" and corresponds to the trace of the product of Fisher's information and the posterior covariance. It is specified as the posterior mean deviance of the model $\overline{D(\theta)}$ minus the point estimate of the model deviance when using the means of the posterior parameter distributions, i.e., $p_D = \overline{D(\theta)} - D(\overline{\theta})$. Thus, with this Bayesian model comparison, we first assess model fit or model "adequacy", $\overline{D(\theta)}$, and then we penalize complexity, p_D. A smaller *DIC* value indicates a "better" model.

Results

Table 1 shows the summary statistics of the observed total *PCB* concentrations in four fish species. Coho salmon had the highest *PCB* concentration (mean 463 and median 410 ng/g wet weight) followed by rainbow trout (mean 399 and median 326 ng/g wet weight), white bass (mean 309 and median 240 ng/g wet weight), and walleye (mean 114 and median 80 ng/g wet weight). Yet, the high standard deviation and interquartile range values reflect the substantial inter- and intra-annual variability associated with the *PCB* levels of the individual fish species. The positive skewness and kurtosis suggest right skewed and leptokurtic distributions; thus, the natural log transformation was implemented for the subsequent modeling analysis, effectively imposing a log-normal error structure on each model.

The posterior estimates for the exponential decay models used to assess the temporal *PCB* trends in walleye *WF* and *SBF* portions are provided in Table 2. The relatively similar *DIC* values between the models with the first and second order temporal smoothing suggest an almost equal support of the two statistical formulations by the observed data. Both approaches predict weakly decreasing trends of the *PCB* concentrations during the study period, while the decay rates were substantially higher in walleye *SBF* ($k \approx -0.040 \text{ yr}^{-1}$) than in *WF* portions ($k = -0.001 \text{ yr}^{-1}$). The predicted mean *PCB* concentrations in the *SBF* portions decreased until the mid 1980s, then remained more or less constant through the early 90s, after which increased until the recent years (Fig. 2a). As previously explained, the δ (random walk) terms were used to detect the systematic errors stemming from the structural inadequacies of the single exponential model. In particular, the positive values of the structural error terms during the second half of the survey period represent the inadequacy of the exponential decay model to capture the concurrent increasing trends (Fig. 2b). By contrast, neither the predicted mean *PCB* patterns show any increasing/decreasing trends throughout the survey period (Fig. 2c), nor the δ terms capture any systematic errors of the model structure for walleye *WF* data (Fig. 2d).

We also examined the robustness of the previous outcomes to the prior distributions assigned to the initial *PCB* concentrations using

Table 3

Sensitivity analysis of the SBF walleye exponential decay model with 1st order random walk using different prior specifications. *Prior 1* and *Prior 2* denote normally and log-normally distributed PCB_0 priors, parameterized such that 95% of the respective values were lying within the minimum and maximum PCB concentrations measured in 1977; and *Prior 3* denotes multivariate normal priors that account for the covariance between the parameters PCB_0 and k.

	Prior 1		Prior 2		Prior 3	
	Mean	SD	Mean	SD	Mean	SD
PCB_0	279	112	322	363	174	89
k	−0.074	0.028	−0.066	0.050	−0.041	0.030
ω	0.592	0.102	0.599	0.104	0.592	0.104
σ_ε	0.776	0.019	0.777	0.019	0.777	0.019
σ_k					0.395	0.525
σPCB_0					211	330
$\sigma k PCB_0$					−62	2142

*σ_k, σ_{PCB_0}, and σk_{PCB_0} represent the three elements of the covariance matrix between the initial *PCB* concentration (PCB_0) and the decay coefficient (k).

Table 4

Posterior estimates of the length (regression) coefficient (mean values ± standard deviations) for the dynamic linear models used to describe the temporal trends of *PCB* concentrations in walleye (both *WF* and *SBF* portions), coho salmon (*SBF*), white bass (*SBF*) and rainbow trout (*SBF*).

| Beta coefficient	Walleye WF		Walleye SBF		Coho salmon SBF		White bass SBF		Rainbow trout SBF	
	DIC_{length} 1702	DIC_{RW} 2007	DIC_{length} 2176	DIC_{RW} 2233	DIC_{length} 1103	DIC_{RW} 1129	DIC_{length} 2060	DIC_{RW} 2501	DIC_{length} 573	DIC_{RW} 628
β_{1977}	0.537 ± 0.095		0.137 ± 0.108		0.187 ± 0.120		0.432 ± 0.090		0.430 ± 0.179	
β_{1978}	0.454 ± 0.035				0.155 ± 0.053		0.047 ± 0.063			
β_{1979}	0.614 ± 0.087		0.171 ± 0.105		0.114 ± 0.086		0.376 ± 0.094			
β_{1980}	0.330 ± 0.065				0.017 ± 0.042		0.473 ± 0.131		0.431 ± 0.173	
β_{1981}	0.247 ± 0.049		0.186 ± 0.090		0.066 ± 0.055		0.875 ± 0.057			
β_{1982}	0.269 ± 0.043		0.289 ± 0.059		0.157 ± 0.059		0.639 ± 0.076			
β_{1983}	0.276 ± 0.066				0.177 ± 0.076		0.358 ± 0.057		0.400 ± 0.165	
β_{1984}	−0.006 ± 0.061		0.208 ± 0.079		0.177 ± 0.063		0.040 ± 0.157			
β_{1985}	0.357 ± 0.067		0.168 ± 0.093		0.135 ± 0.069		0.02 ± 0.032		0.419 ± 0.156	
β_{1986}	0.38 ± 0.076		0.096 ± 0.086		0.094 ± 0.057		0.411 ± 0.114		0.401 ± 0.151	
β_{1987}	0.210 ± 0.110		0.14 ± 0.078		0.136 ± 0.069		0.544 ± 0.073			
β_{1988}	0.113 ± 0.095		0.132 ± 0.066		0.006 ± 0.072		0.606 ± 0.099		0.465 ± 0.149	
β_{1989}	0.073 ± 0.144		0.034 ± 0.079		−0.035 ± 0.098		0.411 ± 0.157			
β_{1990}	0.165 ± 0.106		0.040 ± 0.094		−0.012 ± 0.109		0.308 ± 0.146			
β_{1991}	0.209 ± 0.114		0.165 ± 0.107		0.186 ± 0.132		0.370 ± 0.082			
β_{1992}	0.173 ± 0.108		0.309 ± 0.125				0.242 ± 0.186			
β_{1993}			0.425 ± 0.105				0.329 ± 0.168			
β_{1994}	0.132 ± 0.081		0.376 ± 0.143		0.252 ± 0.121		0.189 ± 0.205		0.390 ± 0.142	
β_{1995}	0.168 ± 0.096				0.318 ± 0.162		0.329 ± 0.211		0.374 ± 0.135	
β_{1996}	0.131 ± 0.132		0.404 ± 0.165				0.431 ± 0.18		0.367 ± 0.133	
β_{1997}	0.123 ± 0.151		0.377 ± 0.189		0.251 ± 0.206		0.181 ± 0.196			
β_{1998}	0.257 ± 0.140		0.361 ± 0.186				0.155 ± 0.209		0.326 ± 0.129	
β_{1999}	0.278 ± 0.220		0.279 ± 0.153				0.236 ± 0.084		0.288 ± 0.122	
β_{2000}	0.251 ± 0.265						0.046 ± 0.249		0.248 ± 0.116	
β_{2001}	0.194 ± 0.254		0.255 ± 0.153				0.064 ± 0.224		0.267 ± 0.106	
β_{2002}	0.141 ± 0.136				0.231 ± 0.27		−0.064 ± 0.182		0.204 ± 0.098	
β_{2003}	0.200 ± 0.158		0.182 ± 0.14				0.292 ± 0.171		0.211 ± 0.084	
β_{2004}	0.122 ± 0.19		0.147 ± 0.133				0.172 ± 0.129		0.146 ± 0.072	
β_{2005}			0.253 ± 0.137				0.643 ± 0.12		0.129 ± 0.053	
β_{2006}	0.275 ± 0.128		0.345 ± 0.146				0.726 ± 0.118		0.113 ± 0.047	
β_{2007}	0.059 ± 0.204		0.324 ± 0.13		0.207 ± 0.341		0.606 ± 0.164		0.157 ± 0.083	

DIC_{length} and DIC_{RW} represent the deviance information criterion values of the dynamic linear models with the fish length as a covariate and their random walk counterparts, respectively.

the first order exponential decay model with the walleye *SBF* data (Table 3). During this sensitivity analysis, the same flat prior distributions were assigned to the decay rates, i.e., $k \sim N(0, 10{,}000)I$ $(,0)$. Prior 2 resulted in relatively higher posterior PCB_0 estimates (322 ± 363 ng *PCB*/g wet weight) followed by Prior 1 (279 ± 112 ng *PCB*/g wet weight) and Prior 3 (174 ± 89 ng *PCB*/g wet weight). Yet, we also note that the use of a log-normally distributed PCB_0 prior (Prior 2) led to a poorly determined posterior estimate. The highest posterior decay coefficients were derived from the Prior 1 ($k = -0.074 \pm 0.028$ yr^{-1}) and Prior 2 ($k = -0.066 \pm 0.050$ yr^{-1}), and the lowest with the Prior 3 ($k = -0.041 \pm 0.030$ yr^{-1}) which was also very similar to the one estimated from the informative normal PCB_0 prior derived from the *PCB* concentrations measured in 1977 (Table 2). Generally, while the measurement error σ_ε and the conditional variance ω associated with the different model specifications were very similar and the inference regarding the presence of a distinct declining trend was unaltered, the actual posterior parameter values appear to be somewhat sensitive to the assumptions made about the PCB_0 prior. Interestingly, the sensitivity exercise also suggests that the PCB_0 and k values tend to covary, i.e., higher PCB_0 estimates are associated with lower k values, although the explicit consideration of such term ($\sigma k PCB_0$) with the Prior 3 has not elucidated the strength of this relationship (-62 ± 2142).

The comparison of the models developed for the four fish species with the *SBF* data suggests that the *PCB* concentrations have been decreasing relatively faster in walleye ($k = -0.040$ and -0.039 yr^{-1} for the first and second order models, respectively), followed by coho salmon ($k = -0.013$ and -0.010 yr^{-1}), white bass ($k = -0.009$ yr^{-1} for both models) and rainbow trout ($k = -0.007$ yr^{-1} for both models).

Similar to the aforementioned results for walleye, the *DIC* values suggest that the first and second order temporal smoothing are almost equally supported by the observed data when we consider both model performance and complexity. The predicted average *PCB* trends in white bass demonstrate a wax and wane pattern throughout the survey period with a net contaminant decrease in recent years (Fig. 2e), while the random walk terms do not reveal any systematic trends unaccounted for by the exponential decay model (Fig. 2f). The *PCB* levels in coho salmon declined gradually from 1976 until the most recent years in our dataset (Fig. 2g), although the actual magnitude of this decreasing trend is hard to be accurately quantified due to extensive data gaps in the 1990s and 2000s. Similarly, the rainbow trout exhibited a net decrease in *PCB* concentrations from 1980s to 2000s, but the inconsistent information from the earlier years of the study period and the lack of data from the mid-90s impedes the precise delineation of the trends followed (Fig. 2i). The δ terms for the latter two species do not suggest any major deviations from the trajectory postulated by the simple exponential decay model (Figs. 2h and j).

The structural flexibility of the *DLMs* allows the model parameters to change over time and also accommodates the covariance between *PCB* concentrations and other potentially important fish characteristics. In a preliminary exploratory analysis, we conducted a model search in which models with identical structures, but different covariates (length, weight, lipid content, gender) were compared on the basis of their difference in log$_e$ likelihoods. Differences in log$_e$ likelihood between identically structured models with different covariates were interpreted as evidence in favor of one covariate over another. In this exercise, the DLM with the fish length outperformed all the rest models. Further, the same models also outperformed their random walk counterparts that do not consider any covariates (see DIC values in Table 4). In the second
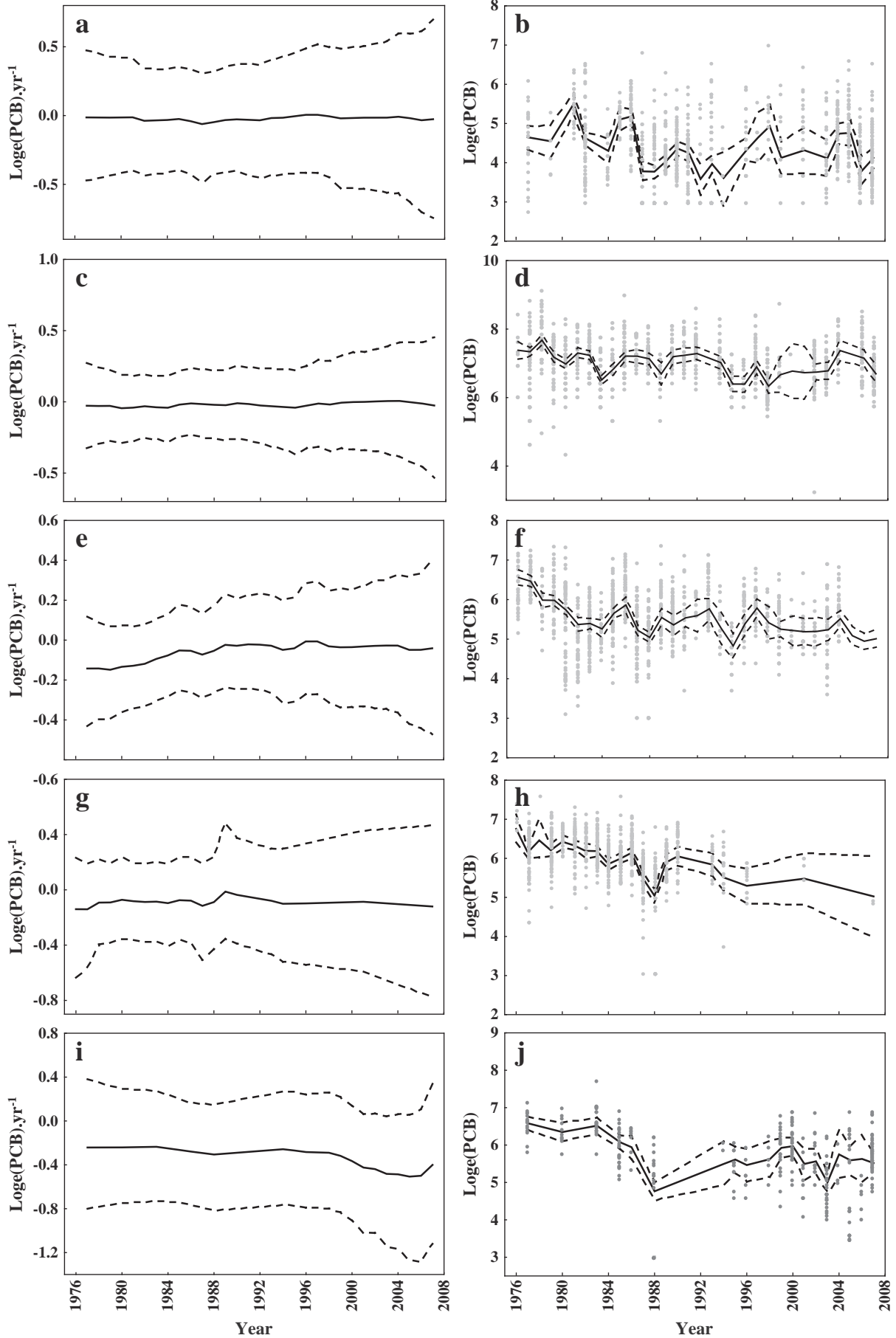
phase, we examined whether the inclusion of a second covariate (along with the fish length) can improve the predictive capacity of our DLM analysis. Aside from the case of walleye *SBF*, the model with the fish length as a single covariate was proven to be the most parsimonious construct (i.e., lowest DIC values) to detect fish contaminant trends in Lake Erie. The *DLM* analysis identified three distinct patterns regarding the rates of change of the *PCB* levels in the fish species examined (Fig. 3). First, the walleye *SBF* and *WF* models show no profound temporal shifts in the rates which remain nearly zero throughout the study period (Figs. 3a and c), and therefore the corrections for the fish length drive the year-to-year variability associated with the level parameter (Figs. 3b and d). Further, the discrepancy between the walleye *SBF* trends when partialling out the covariance with the fish length (Fig. 3b) and the trends from the exponential decay model (Fig. 2b) suggest that the fish sampling practices in Lake Erie may introduce a bias, and therefore a rigorous assessment of contaminant trends in space and time should rather be based on an explicit consideration of the possible covariates (e.g., length, age, gender, lipid content, season). Second, the *PCB* rates of change of the white bass concentrations have switched from weakly negative to nearly zero during the 2000s (Fig. 3e), and the predicted length-adjusted mean *PCB* values appear to have been stabilized after a net decrease during the earlier years of the survey period (Fig. 3f). Third, weakly negative rates of change were apparent for coho salmon and rainbow trout during the entire study period (Figs. 3g and i), reflecting the moderate decrease of the corresponding concentrations. Yet, we caution that the robustness of the latter pattern remains to be confirmed due to the temporal gaps of the information used during the early 90s (Fig. 3j) or the most recent years (Fig. 3h). Finally, aside from the cases in which the sampling bias introduces discrepancies (e.g., walleye *SBF* data), we highlight the remarkable consistency between the trends delineated by the random walk terms of the exponential decay models (lines in the right panels of Fig. 2) and the length-corrected *DLM* predictions (lines in the right panels of Fig. 3).

Discussion

The major sources of toxic substances in Lake Erie have been point discharges from industrial and municipal facilities along with the non-point urban and agricultural runoff. Many of the persistent, bioaccumulative, and toxic organic contaminants are primarily associated with the high organic carbon and fine-grained (silt/clay) fractions of the sediments and thus are mainly transported as part of the sediment load in rivers and tributaries (Marvin et al., 2002). Atmospheric transport and deposition processes can potentially be another significant source of contamination, and existing evidence of *PCB* congener patterns suggests that the contribution of airborne pollutants can dominate the fluxes from other local sources (Datta et al., 1998). In Lake Erie, the lake-wide average *PCB* concentration in the sediments was 43 ng/g in 1997, approximately representing a three-fold decrease since 1971 (Painter et al., 2001). Yet, the Detroit River still appears to be an active contaminant source, whereby more than 70% of the sediment-bound pollutants accumulate in the relatively small western basin within 20–30 km of the mouth of the river (Carter and Hites, 1992). As a result, the local *PCB* fish body burdens are substantially higher, e.g., the average *PCB* levels in walleye *SBF* were approximately 50 ng/g higher in the western relative to the eastern basin during the study period, and therefore any modeling exercise aiming to detect temporal trends of fish contaminants in aggregated datasets should ensure the (reasonably) objective representation of the different locations of the lake. Aside from walleye, the dataset used does not have consistent information

for all the sites to rigorously examine the site-specific temporal trends. In the case of walleye *SBF* though, the development of local dynamic linear models has revealed a more distinctly decreasing trend in the eastern basin relative to the western part of the lake during the earlier years of the study period. Notably, the samples from the eastern part were also characterized from greater mean length (53.29 ± 10.04 cm) and weight (1704 ± 868 g) relative to those collected from the western basin (44.58 ± 8.44 cm and 973 ± 568 g). Thus, the local sampling practices can potentially introduce a systematic bias, which in turn reinforces the need to explicit consider all the possible covariates (e.g., length, gender, lipid content) that can potentially impede the detection of the actual temporal trends of fish contaminants and consequently may misinform consumption advisories.

Depending on their ethology and trophic position, fish are likely to receive *PCBs* through three specific routes, viz., gills, epithelial/dermal tissues and gastrointestinal tract (Schlenk, 2005). Lower trophic level fish primarily receive contaminants by the diffusion process through gills and epithelial cells, whereas top predators primarily receive them through dietary uptake of contaminated food. Sediment can be directly ingested by bottom dwelling aquatic organisms which in turn are the food source for higher aquatic animals. In the western basin of Lake Erie, fish are predicted to accumulate less than half of their contaminant body burden from the sediments, while almost 100% of the fish contaminants directly (i.e., consumption of the bottom sediment) or indirectly (i.e., consumption of organisms that consume sediment or organisms contaminated with sediment) originate from the sediment in the eastern basin (Morrison et al., 2002). Once contaminants are absorbed in the fish body, they can be distributed to specific target organs causing direct biological effects; they may be transported to storage repositories with high lipid content; they may be directly excreted from the body without any interaction with target organs or storage depots; or the lipophilic compounds tend to biotransform to more hydrophilic derivatives in order to enhance polarity and subsequent elimination (Schlenk, 2005).

In our study, the walleye whole fish portions had one order of magnitude higher *PCB* concentrations than the skinless–boneless filet data. Because of their lipophilic and non-polar nature, *PCBs* tend to be deposited in fat tissues and therefore the greater levels in whole fish data are plausible (Elskus et al., 2005). Yet, the significant difference between whole fish and skinless boneless filet data in Lake Erie is somewhat unusual relative to what has been reported (or assumed) in the literature (Jackson and Schindler, 1996; Stow and Carpenter, 1994). For example, Amrhein et al. (1999) reported average whole-fish to filet *PCB* concentration ratios of 1.70 for coho salmon and 1.47 for rainbow trout in Lake Michigan, but these ratios demonstrated substantial variability among individuals and there were also instances characterized by higher concentration in filet than in whole-fish portions. The same study also reported an almost linear relationship between filet and whole fish *PCB* concentrations (see their Fig. 2), which was on par with the typical assumption that trends in filet measurements should also reflect trends in the corresponding whole fish levels (Bhavsar et al., 2007). While our results seem to deviate from both popular notions, we caution that the filet and whole-fish concentrations were not derived from concurrent samples and therefore these discrepancies largely stem from the different philosophies (and associated sampling practices) of the two datasets used (Bhavsar et al., 2010). In particular, while the substantial mobility of walleye can conceivably alleviate the biases associated with the various lake locations sampled each year, the whole-fish samples were almost exclusively collected from Pelee Island in the

Fig. 3. Dynamic Linear Modeling analysis. Left panels depict the annual rates of change of PCB concentrations in (a, b) walleye skinless–boneless filet, (c, d) walleye whole fish, (e, f) white bass skinless–boneless filet, (g, h) coho salmon skinless–boneless filet, and (i, j) rainbow trout skinless–boneless filet data from Lake Erie. Right panels depict the measured *PCB* concentrations (gray dots) against the *PCB* trends when accounting for the covariance with the fish length (black lines). The solid and dashed lines correspond to the median and the 95% credible intervals of the posterior predictive distributions, respectively.
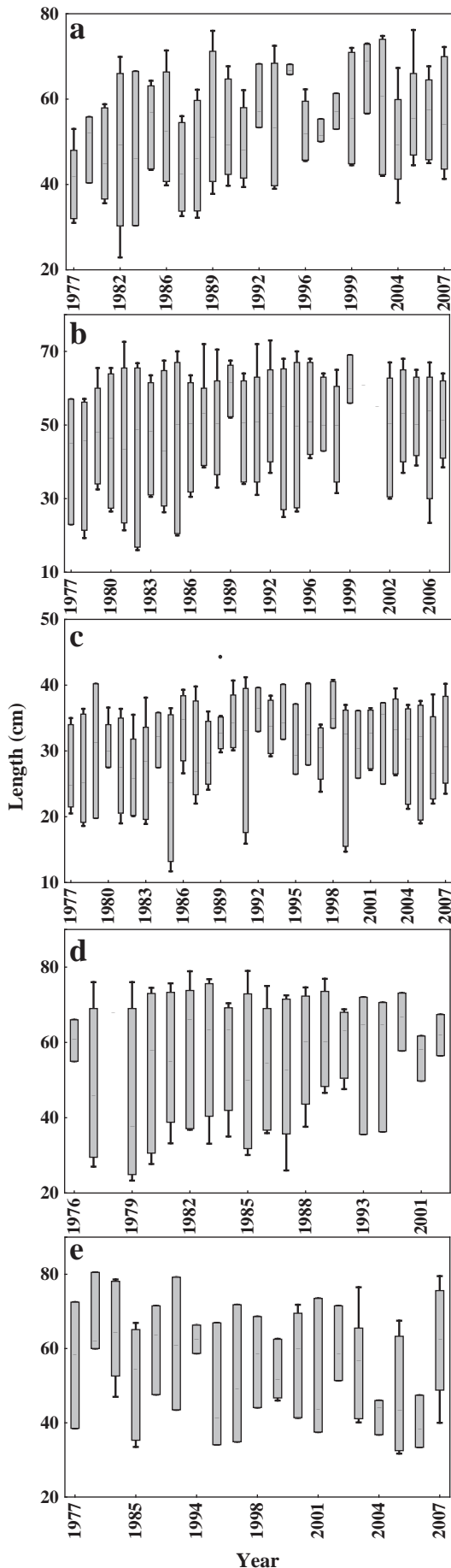
western part of Lake Erie as opposed to the filet data that are based on samples from the entire lake.

Consistent with Bhavsar et al.'s (2007) interpretation of the Lake Erie walleye *SBF* data (see their Fig. 1), our exponential modeling approach suggests that the moderately weak declining rates leveled off since the late 80s and may follow an upward trajectory after the mid-90s. Notably, Bhavsar's study was based on the 45–55 cm size range, which approximately corresponds to the mass of data included within the second and seventh deciles of the dataset used herein. Yet, the dynamic linear modeling analysis appears to negate the previous results, indicating that both the *PCB* rates of change (Fig. 3a) and the corresponding concentrations when explicitly considering their covariance with the fish length (Fig. 3b) do not demonstrate any major trends over the time span examined. The discrepancy between the two modeling approaches stems from the systematic increase of the annual median values of the walleye lengths sampled, which was particularly evident with the filet data (Figs. 4a and b). The same trend was not apparent in the other three species examined in this study (Figs. 4c–e), although the substantial interannual variability of the median length values draws attention to a potential bias if we do not partial out the fish size effects on *PCB* bioaccumulation (Amrhein et al., 1999; Carlson and Swackhamer, 2006). Generally, while the image portrayed from our analysis is somewhat inconclusive with regards to the *PCB* dynamics in walleye over the last three decades, it does certainly cast doubt on the likelihood of achieving the Great Lakes Strategy 2002 objective of 25% decrease in concentrations within a reasonably foreseeable time (Stow et al., 2004; U.S.EPA, 2002). In this regard, our walleye results are again consistent with Bhavsar et al.'s (2007) bootstrap resampling analysis that also ruled out the possibility of compliance with the targeted goals in Lake Erie, although the present analysis does not unequivocally support the same study's projection of an increase in the *PCB* concentrations. This difference between our and Bhavsar et al.'s (2007) trends after the mid-1990s could be attributed to the consideration of more recent data (for years 2006, 2007) in the present study which were among the lowest measurements since the 1990s as well as to the relatively higher variability in measurements relative to the overall low *PCB* levels.

Among the other fish species examined, both the exponential decay and the dynamic linear models suggest that the *PCB* levels in white bass have not undergone any conspicuous changes during the time span examined. Yet, a careful inspection of the observed trends demonstrates an oscillatory pattern which was mainly captured by our exponential model (i.e., Fig. 2e). Similar oscillations are also evident in other Great Lakes time-series for several fish species and have been mainly attributed to the nature and relative strength of the different prey–predator interactions within the aquatic food webs and/or to the periodicities of the climatic forcing (e.g., Borgmann and Whittle, 1991; French et al., 2006; Scheider et al., 1998). Despite the lack of consistent information for coho salmon, both our modeling approaches suggest negative rates of change and continuous decrease of the *PCB* levels during the survey period, although these declining trends are significantly weaker than those reported for the same species in other systems, e.g., Lake Ontario (French et al., 2006). Similarly, the rainbow trout *DLM* suggests weakly decrease of the *PCB* levels, and the odds that the rate parameter has been negative are on average 2.4:1 for coho salmon and 2.3:1 for rainbow trout during the study period. [Note that the odds ratio of the rate parameter being below zero in a particular year is the ratio of the probability mass below zero to the mass above zero.]

Fig. 4. Box plots of the annual sampled length for (a) walleye skinless–boneless filet, (b) walleye whole fish, (c) white bass skinless–boneless filet, (d) coho salmon skinless–boneless filet, and (e) rainbow trout skinless–boneless filet in Lake Erie. Extreme values are not included in these plots.
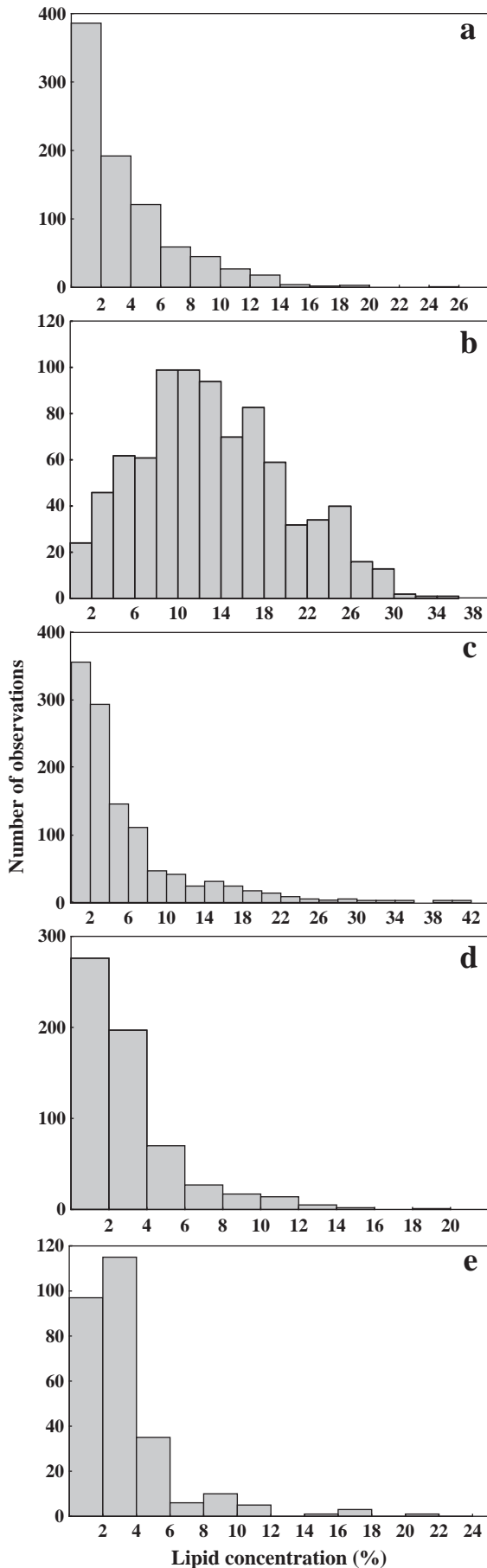
Fig. 5. The lipid concentration frequency distributions of the fish species examined.

Many plausible explanations have been proposed to elucidate the limited response of Lake Erie to the various contamination abatement strategies. One popular hypothesis argues that the decrease in external *PCB* inputs may have altered the contaminant fluxes among the various media (water, atmosphere, sediments), whereby the sediments that historically acted as a net sink for *PCBs* may have switched into a net source (Pearson et al., 1996). Consequently, the signature of the sediment contributions to the *PCB* body burdens is predicted to increase and to ultimately reach a chemical equilibrium between sediments and aquatic biota (Morrison et al., 2002). Given that the profound ecological implication of such equilibrium is the resonance of the corresponding concentrations, the plateau-type of pattern (i.e., a decline in the rate of decrease in *PCB* concentrations in aquatic biota) recently reported in many Great Lakes may partly reflect the relatively static character of the contaminants in the sediments (De Vault et al., 1996; Hickey et al., 2006; Huestis et al., 1996). Yet, this mechanistic explanation of the response of the aquatic biota to the external *PCB* loading reductions may not hold true for the entire Lake Erie due to the significant spatial heterogeneity characterizing the sediment contamination in the system. In particular, despite the substantial decrease of the lakewide average *PCB* concentrations (i.e., from 136 ng/g in 1971 to 43 ng/g in 1997), exceedances of sediment guidelines indicative of contaminated environments still occur in Lake Erie; especially, in the western basin and the southern portion of the central basin (Painter et al., 2001). In eastern Lake Erie, where the fugacity of the various *PCB* congeners in the sediment is significantly higher than their fugacity in the water, the *PCB* body burden of the local biotic communities primarily stems from sediment-bound chemicals (Morrison et al., 2002). Contrary to the predictions of the proposed mechanism though, the prevailing conditions in the western Lake Erie suggest a smaller chemical disequilibrium between the two phases and thus the *PCB* burdens mainly originate from the water column (Morrison et al., 2002). If we also consider that the exchanges between atmosphere and water through wet/dry deposition and volatilization can further modulate the *PCB* fluxes among the various ecosystem components (Jeremiason et al., 1994; Mackay and Bentzen, 1997), the role of the sediments alone may not be sufficient to explain the trajectories delineated by our spatially-integrated models.

Another driving factor that has been hypothesized to underlie the *PCB* temporal trends involves the structural shifts of the Lake Erie food web after the invasion of dreissenids and round gobies in the late 1980s. The invasion of exotic species is hypothesized to have caused a major reconfiguration of the food web from a pelagic-based to a benthic-based one, which in turn has created new trophodynamics for contaminant transfer to top predators (Hogan et al., 2007). First, the introduction of zebra and quagga mussels has likely induced major changes in the *PCB* fluxes within the Lake Erie food web, because of their ability to bioaccumulate by filtering contaminated water and scavenging seston; by directly or indirectly influencing the diet compositions of other biota; and by the selective removal of particulate organic matter from the water column and the subsequent increase of the equilibrium concentrations of the dissolved-phase contaminants which in turn can increase the body burdens of many aquatic organisms (Morrison et al., 1998). Second, round goby invaded the Great Lakes and became extremely abundant in Lake Erie in 1996, causing major shifts in trophic relationships, displacement of native species populations from optimal spawning and feeding habitats, and increased growth rates of top predators (Dubs and Corkum, 1996; Hogan et al., 2007; Ray and Corkum, 1997). As a benthic fish with diet mainly composed of dreissenids and as component of the diets of many commercially and recreationally important species (e.g., walleye, yellow perch, smallmouth bass), round goby has the potential to accumulate contaminants and then transfer them to the higher trophic levels (Johnson et al., 2005). In particular, the benthivorous fish species (e.g., yellow perch and
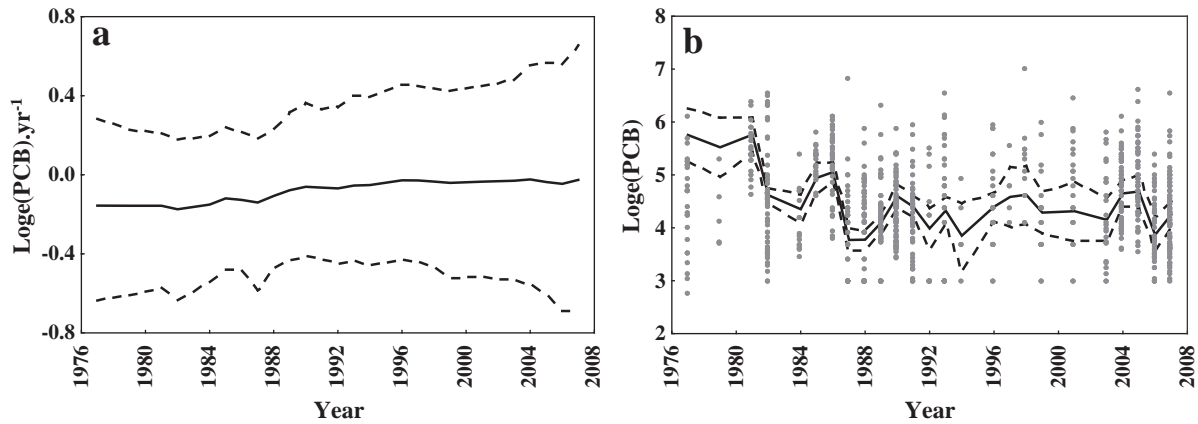
Fig. 6. Annual rates of change (a) and temporal trends (b) of the PCB concentrations, when accounting for the covariance with the fish length and the lipid content in walleye skinless–boneless filet data.

smallmouth bass) have been projected to experience larger increases in their *PCB* burdens due to the effects of round gobies, whereas the impact on pelagic fish species (e.g., alewife and walleye) was relatively smaller (Johnson et al., 2005; Morrison et al., 2000). Our results do not refute the existing predictions regarding the relatively minor change of the walleye *PCB* levels following the invasion of exotic species, and a careful review of the pertinent literature does not provide evidence of strong walleye reliance on round goby (Bur et al., 2008; Jude et al., 2010). Yet, we cannot rule out the existence of indirect trophic paths (e.g., through the impact of round gobies on other prey fishes) that can presumably shape the contaminant patterns in top pelagic predators. In this regard, we also highlight that a concurrent analysis of the total *Hg* variability in the same species does reveal an increasing trend after the mid-90s (Azim et al., 2011).

Aside from the relationship between *PCB* concentrations and fish length, the fish lipid content stands out as one of the possible covariates that have received considerable attention in the literature (Amrhein et al., 1999; Ewald and Larsson, 1994; Rowan and Rasmussen, 1992; Stow, 1995; Voiland et al., 1991). Generally, there are contradictory results regarding the strength of the causal link between fish lipid content and organochlorine contaminant levels (Amrhein et al., 1999; Larsson et al., 1996). In the Lake Erie dataset, if we compare the species-specific *PCB* statistics (Table 1) with their corresponding lipid levels (Fig. 5), we can infer that the lipid content certainly plays a role in contaminant accumulation differences among species. Yet, a preliminary examination (not presented here) of the strength of the *PCB*:lipid relationship among individuals revealed weak covariance for all the fish species studied in our analysis. The only exception was the case of the walleye skinless boneless filet data, in which the most parsimonious dynamic linear model (DIC = 2013) considers both fish length and lipid content as covariates. Yet, the inference drawn from this model remained practically unaltered relative to the model with the fish length as the sole covariate (Fig. 6). The same result was also true when we considered other potentially important covariates, such as the fish age and gender. Stow et al. (1997) reported very similar patterns for five species of Lake Michigan salmonids, but also identified a stronger *PCB*:lipid association when focusing on samples collected during the spawning period (see their Fig. 5). Likewise, Amrhein et al. (1999) found that lipid normalization does not efficiently control within-species variability, but can accentuate among-species differences. Thus, although the reconciliation of the interplay between fish contaminant levels and their lipid content warrants consideration, we underscore that the fish length was the single best covariate for detecting *PCB* temporal trends in Lake Erie.

In conclusion, our analysis shows that the *PCBs* have been decreasing over the last 30 years with relatively weak rates that vary among the different fish species examined. The walleye skinless–boneless filet data are characterized by an increasing trend in the *PCB* concentrations after the mid-90s, which however disappears when explicitly considering the fish length as a covariate. Our *DLM* analysis also suggests that the walleye *WF* trends show no profound changes suggesting relatively stable levels throughout the study period. The coho salmon and rainbow trout *PCB* concentrations have been decreasing steadily during the study period but the associated rates were relatively weak, while the same trends in white bass appear to have been stabilized over that last decade after a weak decrease during the 70s and 80s. The robustness of the latter results remains to be verified due to the temporal gaps and inconsistencies of the information used. The different trends demonstrated by the various fish species herein stress the importance of considering more than one fish species for proper spatial/temporal trend assessments. Finally, we emphasize that the differences between the two phases of our statistical analysis pinpoint the potential bias introduced by all the time-series analysis strategies (single and double exponential decay, mixed order models, simple regression analysis) that do not consider the role of important covariates. Yet, aside from the studies that screened the datasets prior to the analysis and subsequently focused on a specific (narrow) fish length or lipid content range, much of the contemporary literature draws inference on statistical trends that fail to explicitly account for potentially important covariates (e.g., length, age, lipid content, location). One of the take-home messages from our study is that the likelihood of a systematic sampling bias can impede the detection of the actual temporal trends of fish contaminants, and thus may misleadingly guide fish consumption advisories.

Acknowledgments

Appendix A. Supplementary data

Supplementary data to this article can be found online at doi:10.1016/j.jglr.2011.06.005.

References

Amrhein, J.F., Stow, C.A., Wible, C., 1999. Whole-fish versus fillet polychlorinated-biphenyl concentrations: an analysis using classification and regression tree models. Environ. Toxicol. Chem. 18, 1817–1823.

Arhonditsis, G.B., Papantou, D., Zhang, W.T., Perhar, G., Massos, E., Shi, M.L., 2008a. Bayesian calibration of mechanistic aquatic biogeochemical models and benefits for environmental management. J. Mar. Syst. 73, 8–30.

Arhonditsis, G.B., Perhar, G., Zhang, W., Massos, E., Shi, M., Das, A., 2008b. Addressing equifinality and uncertainty in eutrophication models. Water Resour. Res. 44 (W01420, 19 pp.).

Azim, M.E., Kumarappah, A., Bhavsar, S., Backus, S., Arhonditsis, G.B., 2011. Detection of the spatiotemporal trends of mercury contamination in Lake Erie fish communities: a Bayesian approach. Environ. Sci. Technol. 45, 2217–2226.

Bhavsar, S.P., Jackson, D.A., Hayton, A., Reiner, E.J., Chen, T., Bodnar, J., 2007. Are PCB levels in fish from the Canadian Great Lakes still declining? J. Great Lakes Res. 33, 592–605.

Bhavsar, S.P., Gewurtz, S.B., McGoldrick, D.J., Keir, M.J., Backus, S.M., 2010. Changes in mercury levels in Great Lakes fish between 1970s and 2007. Environ. Sci. Technol. 44, 3273–3279.

Borgmann, U., Whittle, D.M., 1983. Particle-size-conversion efficiency and contaminant concentrations in Lake Ontario biota. Can. J. Fish. Aquat. Sci. 40, 328–336.

Borgmann, U., Whittle, D.M., 1991. Contaminant concentration trends in Lake-Ontario lake trout (Salvelinus nmaycush) — 1977 to 1988. J. Great Lakes Res. 17, 368–381.

Brooks, S.P., Gelman, A., 1998. General methods for monitoring convergence of iterative simulations. J. Comput. Graph. Stat. 7, 434–455.

Bur, M.T., Stapanian, M.A., Bernhardt, G., Turner, M.W., 2008. Fall diets of red-breasted merganser (Mergus serrator) and walleye (Sander vitreus) in Sandusky Bay and adjacent waters of Western Lake Erie. Am. Midl. Nat. 159, 147–161.

Carlson, D.L., Swackhamer, D.L., 2006. Results from the US Great Lakes fish monitoring program and effects of lake processes on bioaccumulative contaminant concentrations. J. Great Lakes Res. 32, 370–385.

Carlson, D.L, De Vault, D., Swackhamer, D., 2010. On the rate of decline of persistent organic contaminants in lake trout (Salvelinus namaycush) from the Great Lakes, 1970–2003. Environ. Sci. Technol. 44, 2004–2010.

Carter, D.S., Hites, R.A., 1992. Fate and transport of Detroit River drived pollutants throughout Lake Erie. Environ. Sci. Technol. 26, 1333–1341.

Cole, D.C., Kearney, J., Sanin, L.H., Leblanc, A., Weber, J.P., 2004. Blood mercury levels among Ontario anglers and sport-fish eaters. Environ. Res. 95, 305–314.

Datta, S., McConnell, L.L., Baker, J.E., Lenoir, J., Seiber, J.N., 1998. Evidence for atmospheric transport and deposition of polychlorinated biphenyls to the Lake Tahoe basin, California – Nevada. Environ. Sci. Technol. 32, 1378–1385.

De Vault, D.S., Hesselberg, R., Rodgers, P.W., Feist, T.J., 1996. Contaminant trends in lake tout and walleye from the Laurentian Great Lakes. J. Great Lakes Res. 22, 884–895.

Dubs, D.O.L., Corkum, L.D., 1996. Behavioural interactions between round gobies (Neogobius melanostomus) and mottled sculpins (Cottus bairdi). J. Great Lakes Res. 22, 838–844.

Elskus, A.A., Coller, T.K., Monosson, E., 2005. Interactions between lipids and persistent organic pollutants in fish. In: Mommsen, T.P., Moon, T.W. (Eds.), Biochemistry and Molecular Biology of Fishes, vol. 6. Elsevier BV, pp. 119–152.

Ewald, G., Larsson, P., 1994. Partitioning of ^{14}C-labelled 2,2',4,4'-tetrachlorobiphenyl between water and fish lipids. Environ. Toxicol. Chem. 13, 1577–1580.

Faroon, O., Jones, D., De Rosa, C., 2000. Effects of polychlorinated biphenyls on the nervous system. Toxicol. Ind. Health 16, 307–333.

Fitzgerald, E.F., Belanger, E.E., Gomez, M.I., Cayo, M., McCaffrey, R.J., Seegal, R.F., Jansing, R.L., Hwang, S.A., Hicks, H.E., 2008. Polychlorinated biphenyl exposure and neuropsychological status among older residents of upper Hudson River communities. Environ. Health Perspect. 116, 209–215.

French, T.D., Campbell, L.M., Jackson, D.A., Casselman, J.M., Scheider, W.A., Hayton, A., 2006. Long-term changes in legacy trace organic contaminants and mercury in Lake Ontario salmon in relation to source controls, trophodynamics, and climatic variability. Limnol. Oceanogr. 51, 2794–2807.

Gelman, A., Carlin, J.B., Stern, H.S., Rubin, D.B., 2004. Bayesian Data Analysis, Second ed. Chapman & Hall, New York.

Gewurtz, S.B., Bhavsar, S.P., Jackson, D.A., Fletcher, R., Awad, E., Moody, R., Reiner, E.A., 2010. Temporal and spatial trends of organochlorines and mercury in fishes from the St. Clair River/Lake St. Clair corridor, Canada. J. Great Lakes Res. 36, 100–112.

Gilks, W., Roberts, G.O., Sahu, S.K., 1998. Adaptive Markov Chain Monte Carlo through regeneration. J. Am. Stat. Assoc. 93, 1045–1054.

Hickey, J.P., Batterman, S.A., Chernyak, S.M., 2006. Trends of chlorinated organic contaminants in Great Lakes trout and walleye from 1970 to 1998. Arch. Environ. Contam. Toxicol. 50, 97–110.

Hogan, L.S., Marschall, E., Folt, C., Stein, R.A., 2007. How non-native species in Lake Erie influence trophic transfer of mercury and lead to top predators. J. Great Lakes Res. 33, 46–61.

Huestis, S.Y., Servos, M.R., Whittle, D.M., Dixon, D.G., 1996. Temporal and age-related trends in levels of polychlorinated biphenyl congeners and organochlorine contaminants in Lake Ontario lake trout (Salvelinus namaycush). J. Great Lakes Res. 22, 310–330.

Humphrey, H.E.B., 1988. Chemical contaminants in the Great Lakes: the human health aspects. In: Evans, M.S. (Ed.), Toxic Contaminants and Ecosystem Health: A Great Lakes Focus. Wiley Inter Science, New York, pp. 153–168.

International Joint Commission (IJC), 1978. Great Lakes Water Quality Agreement as Amended by Protocol. Windsor, ON, Canada.

International Joint Commission (IJC), 2006. A Guide to the Great Lakes Water Quality Agreement: Background for the 2006 Governmental Review. 1-894280-53-9. Canada and the United States.

Jackson, L.J., Schindler, D.E., 1996. Field estimates of net trophic transfer of PCBs from prey fishes to Lake Michigan salmonids. Environ. Sci. Technol. 30, 1861–1865.

Jeremiason, J.D., Hornbuckle, K.C., Eisenreich, S.J., 1994. PCBS in Lake-Superior, 1978–1992 — decreases in water concentrations reflect loss by volatilization. Environ. Sci. Technol. 28, 903–914.

Johnson, B.L., Hicks, H.E., De Rosa, C.T., 1999. Key environmental human health issues in the Great Lakes and St. Lawrence River basins. Environ. Res. 80, S2–S12.

Johnson, T.B., Bunnell, D.B., Knight, C.T., 2005. A potential new energy pathway in central Lake Erie: the round goby connection. J. Great Lakes Res. 31 (Suppl. 2), 238–251.

Jude, D.J., Rediske, R., O'Keefe, J., Hensler, S., Giesy, J.P., 2010. PCB concentrations in walleyes and their prey from the Saginaw River, Lake Huron: a comparison between 1990 and 2007. J. Great Lakes Res. 36, 267–276.

Lamon, E.C., Carpenter, S.R., Stow, C.A., 1998. Forecasting PCB concentrations in Lake Michigan salmonids: a dynamic linear model approach. Ecol. Appl. 8, 659–668.

Larsson, P., Backe, C., Bremle, G., Eklöv, A., Okla, L., 1996. Persistent pollutants in a salmon population (Salmo salar) of the southern Baltic Sea. Can. J. Fish. Aquat. Sci. 53, 62–69.

Mackay, D., Bentzen, E., 1997. The role of the atmosphere in Great Lakes contamination. Atmos. Environ. 31, 4045–4047.

Marvin, C., Alaee, M., Painter, S., Charlton, M., Kauss, P., Kolic, T., MacPherson, K., Takeuchi, D., Reiner, E., 2002. Persistent organic pollutants in Detroit River suspended sediments: polychlorinated dibenzo-p-dioxins and dibenzofurans, dioxin-like polychlorinated biphenyls and polychlorinated naphthalenes. Chemosphere 49, 111–120.

Morrison, H.A., Gobas, F., Lazar, R., Whittle, D.M., Haffner, G.D., 1998. Projected changes to the trophodynamics of PCBs in the western Lake Erie ecosystem attributed to the presence of zebra mussels (Dreissena polymorpha). Environ. Sci. Technol. 32, 3862–3867.

Morrison, H.A., Whittle, D.M., Haffner, G.D., 2000. The relative importance of species invasions and sediment disturbance in regulating chemical dynamics in western Lake Erie. Ecol. Model. 125, 279–294.

Morrison, H.A., Whittle, D.M., Haffner, G.D., 2002. A comparison of the transport and fate of polychlorinated biphenyl congeners in three Great Lakes food webs. Environ. Toxicol. Chem. 21, 683–692.

Painter, S., Marvin, C., Rosa, F., Reynoldson, T.B., Charlton, M.N., Fox, M., Thiessen, L., Estenik, J.F., 2001. Sediment contamination in Lake Erie: a 25-year retrospective analysis. J. Great Lakes Res. 27, 434–448.

Pearson, R.F., Hornbuckle, K.C., Eisenreich, S.J., Swackhamer, D.L., 1996. PCBs in Lake Michigan water revisited. Environ. Sci. Technol. 30, 1429–1436.

Pole, A., West, M., Harrison, J., 1994. Applied Bayesian Forecastingand Time Series Analysis. Chapman & Hall, New York.

Ray, W.J., Corkum, L.D., 1997. Predation of zebra mussels by round gobies, Neogobius melanostomus. Environ. Biol. Fish. 50, 267–273.

Rowan, D.J., Rasmussen, J.B., 1992. Why don't Great Lakes fish reflect environmental concentrations of organic contaminants — an analysis of between-lake variability in the ecological partitioning of PCBs and DDT. J. Great Lakes Res. 18, 724–741.

Scheider, W.A., Cox, C., Hayton, A., Hitchin, G., 1998. Current status and temporal trends in concentrations of persistent toxic substances in sport fish and juvenile forage fish in the Canadian waters of the Great Lakes. Environ. Monit. Assess. 53, 57–76.

Schlenk, D., 2005. Pesticide biotransformation in fish. In: Mommsen, T.P., Moon, T.W. (Eds.), Biochemistry and Molecular Biology of Fishes, vol. 6. Elsevier BV, pp. 171–190.

Shaddick, G., Wakefield, J., 2002. Modelling daily multivariate pollutant data at multiple sites. J. R. Stat. Soc. Ser. C App. Stat. 51, 351–372.

Spiegelhalter, D.J., Best, N.G., Carlin, B.R., van der Linde, A., 2002. Bayesian measures of model complexity and fit. J. R. Stat. Soc. Ser. B Stat. Methodol. 64, 583–616.

Stow, C.A., 1995. Factors associated with PCB concentrations in Lake-Michigan salmonids. Environ. Sci. Technol. 29, 522–527.

Stow, C.A., Carpenter, S.R., 1994. PCB accumulation in Lake-Michigan coho and chinook salmon — individual-based models using allometric relationships. Environ. Sci. Technol. 28, 1543–1549.

Stow, C.A., Jackson, L.J., Amrhein, J.F., 1997. An examination of the PCB:lipid relationship among individual fish. Can. J. Fish. Aquat. Sci. 54, 1031–1038.

Stow, C.A., Lamon, E.C., Qian, S.S., Schrank, C.S., 2004. Will Lake Michigan lake trout meet the Great Lakes strategy 2002 PCB reduction goal? Environ. Sci. Technol. 38, 359–363.

Tanabe, S., 1988. PCB problems in the future-foresight from current knowledge. Environ. Pollut. 50, 5–28.

Tee, P.G., Sweeney, A.M., Symanski, E., Gardiner, J.C., Gasior, D.M., Schantz, S.L., 2003. A longitudinal examination of factors related to changes in serum polychlorinated biphenyl levels. Environ. Health Perspect. 111, 702–707.

Tomasallo, C., Anderson, H., Haughwout, M., Imm, P., Knobeloch, L., 2010. Mortality among frequent consumers of Great Lakes sport fish. Environ. Res. 110, 62–69.

Turyk, M.E., Anderson, H.A., Freels, S., Chatterton, R., Needham, L.L., Patterson, D.G., Steenport, D.N., Knobeloch, L., Imm, P., Persky, V.W., 2006. Associations of organochlorines with endogenous hormones in male Great Lakes fish consumers and non-consumers. Environ. Res. 102, 299–307.

Turyk, M., Anderson, H., Knobeloch, L., Imm, P., Persky, V., 2009a. Organochlorine exposure and incidence of diabetes in a cohort of Great Lakes sport fish consumers. Environ. Health Perspect. 117, 1076–1082.

Turyk, M., Anderson, H.A., Knobeloch, L., Imm, P., Persky, V.W., 2009b. Prevalence of diabetes and body burdens of polychlorinated biphenyls, polybrominated diphenyl ethers, and p, p′-diphenyldichloroethene in Great Lakes sport fish consumers. Chemosphere 75, 674–679.

U.S. EPA, 2002. Great Lakes Strategy 2002 available at http://www.epa.gov/glnpo/gls/glstoc.html Office of Water, U.S.EPA., Washington, DC.

Voiland Jr., M.P., Gall, K.L., Lisk, D.J., MacNeill, D.B., 1991. Effectiveness of recommended fat-trimming procedures on the reduction of PCB and Mirex levels in brown trout (*Salmo trutta*) from Lake Ontario. J. Great Lakes Res. 17, 454–460.

West, M., Harrison, P.J., 1989. Bayesian Forecasting and Dynamic Models. Springer-Verlag, New York.

A BAYESIAN ASSESSMENT OF THE PCB TEMPORAL TRENDS IN LAKE ERIE FISH COMMUNITIES

(Electronic Supplementary Material)

Somayeh Sadraddini[1], M. Ekram Azim[1], Yuko Shimoda[1], Satyendra P. Bhavsar[2,3,4], Ken G. Drouillard[4], Sean M. Backus[5], and George B. Arhonditsis[1,3*]

[1] Ecological Modeling Laboratory
Department of Physical and Environmental Sciences
University of Toronto, Toronto, Ontario, M1C 1A4, Canada

[2] Ontario Ministry of Environment, Environmental Monitoring and Reporting Branch
Toronto, Ontario, M9P 3V6, Canada

[3] Centre for Environment
University of Toronto, Toronto, Ontario M5S 3E8

[4] Great Lakes Institute for Environmental Research
University of Windsor, Windsor, Ontario, N9B 3P4, Canada

[5] Water Quality Monitoring & Surveillance Division, Water Science and Technology Directorate
Environment Canada, Burlington, Ontario L7R 4A6

*Corresponding author

E-mail: georgea@utsc.utoronto.ca; Tel: +1 416-208-4858; Fax: +1 416-287-7279

A) The WinBUGS codes associated with all the single exponential decay models of the walleye skinless

boneless fillet data are as follows:

1) Original approach: Non-informative (flat) prior distributions for the parameters PCB_0 and k.

a) First-order temporal smoothing

```
model {

for (i in 1:N) {
LogPCBmod[i]<-log(PCB0*exp(k*time[i]))
LogPCBm[i]<-LogPCBmod[i]+delta[time[i]+1]
LogPCB[i]~dnorm(LogPCBm[i],mtau)
LogPredPCB[i]~dnorm(LogPCBm[i],mtau)
PredPCB[i]<-exp(LogPredPCB[i])}
delta[1:31]~car.normal(adj[],weights[],num[],tau)
        for (i in 1:1)  {
        weights[i]<-1;  adj[i]<-i+1 num[i]<-1}
        for (i in 2:30) {
        weights[2+(i-2)*2]<-1;  adj[2+(i-2)*2]<-i-1;
        weights[3+(i-2)*2]<-1;  adj[3+(i-2)*2]<-i+1; num[i]<-2}
        for (i in 31:31) {
        weights[(i-2)*2+2]<-1;  adj[(i-2)*2+2]<-i-1; num[i]<-1}
mtau~dgamma(0.001,0.001)
msigma<-sqrt(1/mtau)
k~dnorm(0,0.0001)I(,0)
PCB0~dnorm(0,0.0001)I(0,)
tau~dgamma(0.001,0.001)
sigma<-sqrt(1/tau)
}
```

b) Second-order temporal smoothing

```
model {

for (i in 1:N) {
LogPCBmod[i]<-log(PCB0*exp(k*time[i]))
LogPCBm[i]<-LogPCBmod[i]+delta[time[i]+1]
LogPCB[i]~dnorm(LogPCBm[i],mtau)
LogPredPCB[i]~dnorm(LogPCBm[i],mtau)
PredPCB[i]<-exp(LogPredPCB[i])}
delta[1:31]~car.normal(adj[],weights[],num[],tau)
        for (i in 1:1) {
        weights[i] <- 2; adj[i] <- i+1
        weights[i+1] <- -1; adj[i+1] <- i+2; num[i] <- 2}
        for (i in 2:2) {
        weights[i+1] <- 2; adj[i+1] <- i-1
```

```
            weights[i+2] <- 4; adj[i+2] <- i+1
            weights[i+3] <- -1; adj[i+3] <- i+2; num[i] <- 3}
            for (i in 3:29) {
            weights[6+(i-3)*4] <- -1; adj[6+(i-3)*4] <- i-2
            weights[7+(i-3)*4] <- 4; adj[7+(i-3)*4] <- i-1
            weights[8+(i-3)*4] <- 4; adj[8+(i-3)*4] <- i+1
            weights[9+(i-3)*4] <- -1; adj[9+(i-3)*4] <- i+2; num[i] <- 4}
            for (i in 30:30) {
            weights[(31-4)*4 + 6] <- 2; adj[(31-4)*4 + 6] <- i+1
            weights[(31-4)*4 + 7] <- 4; adj[(31-4)*4 + 7] <- i-1
            weights[(31-4)*4 + 8] <- -1; adj[(31-4)*4 + 8] <- i-2; num[i] <- 3}
            for (i in 31:31) {
            weights[(31-4)*4 + 9] <- 2; adj[(31-4)*4 + 9] <- i-1
            weights[(31-4)*4 + 10] <- -1; adj[(31-4)*4 + 10] <- i-2; num[i] <- 2}
mtau~dgamma(0.001,0.001)
msigma<-sqrt(1/mtau)
k~dnorm(0,0.0001)I(,0)
PCB0~dnorm(0,0.0001)I(0,)
tau~dgamma(0.001,0.001)
sigma<-sqrt(1/tau)
}
```

2) *Prior 1:* Normal PCB_0 prior distribution parameterized such that 95% of the respective values lay within the minimum and maximum PCB concentrations in the first year examined.

```
model {

for (i in 1:N) {
LogPCBmod[i]<-log(PCB0*exp(k*time[i]))
LogPCBm[i]<-LogPCBmod[i]+delta[time[i]+1]
LogPCB[i]~dnorm(LogPCBm[i],mtau)
LogPredPCB[i]~dnorm(LogPCBm[i],mtau)
PredPCB[i]<-exp(LogPredPCB[i])}
delta[1:31]~car.normal(adj[],weights[],num[],tau)
            for (i in 1:1)  {
            weights[i]<-1;  adj[i]<-i+1 num[i]<-1}
            for (i in 2:30) {
            weights[2+(i-2)*2]<-1;  adj[2+(i-2)*2]<-i-1;
            weights[3+(i-2)*2]<-1;  adj[3+(i-2)*2]<-i+1; num[i]<-2}
            for (i in 31:31) {
            weights[(i-2)*2+2]<-1;  adj[(i-2)*2+2]<-i-1; num[i]<-1}
mtau~dgamma(0.001,0.001)
msigma<-sqrt(1/mtau)
k~dnorm(0,0.0001)I(,0)
PCB0~dnorm(233,0.0000816)I(0,)
tau~dgamma(0.001,0.001)
sigma<-sqrt(1/tau)
```

}

3) Prior 2: Lognormal _PCB_$_0$ prior distribution parameterized such that 95% of the respective values lay

within the minimum and maximum _PCB_ concentrations in the first year examined.

```
model {

for (i in 1:N) {
LogPCBmod[i]<-log(PCB0*exp(k*time[i]))
LogPCBm[i]<-LogPCBmod[i]+delta[time[i]+1]
LogPCB[i]~dnorm(LogPCBm[i],mtau)
LogPredPCB[i]~dnorm(LogPCBm[i],mtau)
PredPCB[i]<-exp(LogPredPCB[i])}
delta[1:31]~car.normal(adj[],weights[],num[],tau)
        for (i in 1:1)  {
        weights[i]<-1;  adj[i]<-i+1 num[i]<-1}
        for (i in 2:30) {
        weights[2+(i-2)*2]<-1;  adj[2+(i-2)*2]<-i-1;
        weights[3+(i-2)*2]<-1;  adj[3+(i-2)*2]<-i+1; num[i]<-2}
        for (i in 31:31) {
        weights[(i-2)*2+2]<-1;  adj[(i-2)*2+2]<-i-1; num[i]<-1}
mtau~dgamma(0.001,0.001)
msigma<-sqrt(1/mtau)
k~dnorm(0,0.0001)I(,0)
PCB0<-exp(LnPCB0)
LnPCB0~dnorm(4.441,1.3801699)
tau~dgamma(0.001,0.001)
sigma<-sqrt(1/tau)
}
```

4) Prior 3: Multivariate normal prior accounting for the covariance between the parameters _PCB_$_0$ and _k._

```
model {

for (i in 1:N) {
LogPCBmod[i]<-log(PCB0*exp(k*time[i]))
LogPCBm[i]<-LogPCBmod[i]+delta[time[i]+1]
LogPCB[i]~dnorm(LogPCBm[i],mtau)
LogPredPCB[i]~dnorm(LogPCBm[i],mtau)
PredPCB[i]<-exp(LogPredPCB[i])}
delta[1:31]~car.normal(adj[],weights[],num[],tau)
        for (i in 1:1)  {
        weights[i]<-1;  adj[i]<-i+1 num[i]<-1}
        for (i in 2:30) {
        weights[2+(i-2)*2]<-1;  adj[2+(i-2)*2]<-i-1;
        weights[3+(i-2)*2]<-1;  adj[3+(i-2)*2]<-i+1; num[i]<-2}
        for (i in 31:31) {
```

```
        weights[(i-2)*2+2]<-1;  adj[(i-2)*2+2]<-i-1; num[i]<-1}
mtau~dgamma(0.001,0.001)
msigma<-sqrt(1/mtau)
theta[1:2] ~ dmnorm(dmu[1:2], dtau[1:2, 1:2])I(P[],Q[])
dtau[1:2, 1:2] ~ dwish(R[1:2, 1:2], 2)
dsigma2[1:2, 1:2] <- inverse(dtau[1:2, 1:2])
for (i in 1:2) {dsigma[i] <- sqrt(dsigma2[i, i])}
k<-theta[1]
PCB0<-theta[2]
tau~dgamma(0.001,0.001)
sigma<-sqrt(1/tau)
}
```

B) The WinBUGS code associated with the dynamic linear model for the PCB concentrations in walleye skinless boneless fillet data is as follows:

```
model {
# Specification of the observation equation
for (i in 1:N) {
LogPCBm[i]<-level[time[i]+1]+beta[time[i]+1]*length[i]
LogPCB[i]~dnorm(LogPCBm[i],mtau[time[i]+1])
LogPredPCB[i]~dnorm(LogPCBm[i],mtau[time[i]+1])
PredPCB[i]<-exp(LogPredPCB[i])}
# Specification of the system equations for the second year until the end of the study period
for (t in 2:24) {
beta[year[t]]~dnorm(beta[year[t-1]],btau[year[t]])
rate[year[t]]~dnorm(rate[year[t-1]],gtau[year[t]])
levelm[year[t]]<-level[year[t-1]]+rate[year[t]]
level[year[t]]~dnorm(levelm[year[t]],ltau[year[t]])
# Specification of the discount factors for the second year until the end of the study period
ltau[year[t]]<-ltau.in*pow(0.95,year[t]-1)
lsigma[year[t]]<-sqrt(1/ltau[year[t]])
btau[year[t]]<-btau.in*pow(0.95,year[t]-1)
bsigma[year[t]]<-sqrt(1/btau[year[t]])
gtau[year[t]]<-gtau.in*pow(0.95,year[t]-1)
gsigma[year[t]]<-sqrt(1/gtau[year[t]])
mtau[year[t]]<-mtau.in*pow(0.95,year[t]-1)
msigma[year[t]]<-sqrt(1/mtau[year[t]])
}
# Specification of the system equations for the first year
beta[year[1]]~dnorm(beta[1],btau[year[1]])
rate[year[1]]~dnorm(rate[1],gtau[year[1]])
levelm[year[1]]<-level[1]+growth[year[1]]
level[year[1]]~dnorm(levelm[year[1]],ltau[year[1]])
# Specification of the discount factors for the first year
ltau[year[1]]<-ltau.in*pow(0.95,year[1]-1)
```

```
lsigma[year[1]]<-sqrt(1/ltau[year[1]])
btau[year[1]]<-btau.in*pow(0.95,year[1]-1)
bsigma[year[1]]<-sqrt(1/btau[year[1]])
gtau[year[1]]<-gtau.in*pow(0.95,year[1]-1)
gsigma[year[1]]<-sqrt(1/gtau[year[1]])
mtau[year[1]]<-mtau.in*pow(0.95,year[1]-1)
msigma[year[1]]<-sqrt(1/mtau[year[1]])
# Prior distributions for the parameters of the first year
beta[1]~dnorm(0,0.0001)
rate[1]~dnorm(0,0.0001)
level[1]~dnorm(0,0.0001)
ltau.in~dgamma(0.001,0.001)
ltau[1]<-ltau.in
btau.in~dgamma(0.001,0.001)
btau[1]<-btau.in
gtau.in~dgamma(0.001,0.001)
gtau[1]<-gtau.in
mtau.in~dgamma(0.001,0.001)
mtau[1]<-mtau.in

}
```

Inference Data
```
list(N=899,
year=c(3,5,6,8,9,10,11,12,13,14,15,16,17,18,20,21,22,23,25,27,28,29,30,31),
time=c(paste time.dat here),
LogPCB=c(paste walleyePCB.dat here),
length=c(paste length.dat here),
```

Initial values 1
```
list(beta=c(0,NA,0,NA,0,0,NA,0,0,0,0,0,0,0,0,0,0,0,NA,0,0,0,0,NA,0,NA,0,0,0,0,0),
    rate=c(0,NA,0,NA,0,0,NA,0,0,0,0,0,0,0,0,0,0,0,NA,0,0,0,0,NA,0,NA,0,0,0,0,0),
    level=c(0,NA,0,NA,0,0,NA,0,0,0,0,0,0,0,0,0,0,0,NA,0,0,0,0,NA,0,NA,0,0,0,0,0),
    mtau.in=0.2, ltau.in=1, btau.in=1, gtau.in=1,
    LogPredPCB=c(paste walleyePCB.dat here))
```

Initial values 2
```
list(beta=c(1,NA,1,NA,1,1,NA,1,1,1,1,1,1,1,1,1,1,1,NA,1,1,1,1,NA,1,NA,1,1,1,1,1),
    rate=c(1,NA,1,NA,1,1,NA,1,1,1,1,1,1,1,1,1,1,1,NA,1,1,1,1,NA,1,NA,1,1,1,1,1),
    level=c(1,NA,1,NA,1,1,NA,1,1,1,1,1,1,1,1,1,1,1,NA,1,1,1,1,NA,1,NA,1,1,1,1,1),
    mtau.in=0.32, ltau.in=0.32, btau.in=0.32, gtau.in=0.32,
    LogPredPCB=c(paste walleyePCB.dat here)
```